Printed photonic arrays from self-organized chiral nematic liquid crystals

Citation for published version:
Gardiner, DJ, Hsiao, W-K, Morris, SM, Hands, PJW, Wilkinson, TD, Hutchings, IM & Coles, HJ 2012, 'Printed photonic arrays from self-organized chiral nematic liquid crystals' Soft Matter, vol 8, no. 39, pp. 9977-9980. DOI: 10.1039/c2sm26479j

Digital Object Identifier (DOI):
10.1039/c2sm26479j

Published In:
Soft Matter

View Online / Journal Homepage / Table of Contents for this issue
Soft Matter
Dynamic Article Links

Cite this: *Soft Matter*, 2012, **8**, 9977

www.rsc.org/softmatter

COMMUNICATION

Printed photonic arrays from self-organized chiral nematic liquid crystals

D. J. Gardiner,*[a] W.-K. Hsiao,*[b] S. M. Morris,[a] P. J. W. Hands,[a] T. D. Wilkinson,[a] I. M. Hutchings[b] and H. J. Coles*[a]

Received 26th June 2012, Accepted 15th August 2012
DOI: 10.1039/c2sm26479j

Active laser arrays, of arbitrary pattern, were created by inkjet deposition of self-assembled photonic structures in the form of dye-doped chiral nematic liquid crystals. The print process itself achieves the requisite alignment for photonic band-edge lasing action normal to the substrate; laser threshold and linewidth characteristics are presented.

Introduction

Chiral nematic liquid crystals (LCs) are a unique class of functional photonic materials with applications ranging from bistable displays to lasers.[1,2] In these materials, the constituent elongated molecules self-organize into a helicoidal arrangement. The periodic variation of the refractive index generates a photonic band-gap (PBG) for visible wavelengths.[3] This has received significant interest in the context of photonic band-edge lasing,[2,4] since incorporation of an organic fluorescent dye, as the gain medium, into the helical structure can lead to laser emission at the band-edges. Such systems offer high slope efficiency, greater than 60%, narrow linewidth emission[5] and, with the self-organized "soft" periodic structure, broadband wavelength selectivity and tuneability. Typical laser emission wavelengths range from 450 nm to 850 nm.[6–8]

Conventional materials used in most modern laser systems, such as active glasses and semiconductor diodes, are solid-state devices that are incompatible with print deposition technologies, such as roll-to-roll, bar coating or inkjet processing, for example. Semiconductor lasers are typically manufactured using a complex process involving a combination of deposition, etching and photolithography on high quality semiconductor wafers. However, we have previously demonstrated printable emulsion-based LC laser systems that could be deposited using bar coating techniques.[9,10] Therefore, lasing LC media also offer significant potential not only for reducing manufacturing cost, but also to form laser coatings on surfaces, or devices, currently inaccessible to traditional processing.

Whilst offering a facile fabrication process, the disadvantages of bar-coated emulsion based LC laser films are that the size of the individual laser droplets produced are polydisperse, typically of 10's to 100's μm diameter, and are randomly distributed in space. A more functional and flexible approach is to use a direct writing process, such as inkjet printing. Such processes have been investigated as flexible fabrication methods for electronics and biological devices.[11,12] In this work, we describe a "drop-on-demand" inkjet deposition approach that gives precise control of the droplet size and allows the formation of spatially localized laser sources. By depositing the LC lasing material on to a wet, solution-based polymer, the necessary alignment of the LC is obtained. Following optical excitation at the absorption maximum of the laser dye, single-mode laser emission is observed with a well defined threshold and narrow linewidth. The results demonstrate the possibility of creating truly two-dimensional laser arrays of controlled and arbitrary size, position, and wavelength for use in a diverse range of applications.

Experimental

To prepare the liquid crystal (LC) host, 4.2 wt% of the chiral additive BDH-1281 (Merck KGaA), was added to the achiral nematic LC BL006 (Merck KGaA) to generate the chiral nematic phase. This LC possesses a wide temperature range nematic phase with a nematic to isotropic transition temperature of 120 °C. The high quantum efficiency laser dye, Pyrromethene-597 (obtained from Exciton), was added to the chiral nematic mixture at a concentration of 1 wt%. Mixtures were placed in an oven for a period of 24 hours at 10 °C above the nematic to isotropic transition temperature to ensure sufficient thermal diffusion of the constituents. In order to confirm the position of the long-wavelength photonic band-edge, which defines the laser wavelength of the LC droplet, mixtures were capillary filled into 10 μm thickness glass cells, which had antiparallel rubbed polyimide alignment layers.

For the inkjet deposition study, 10 wt% polyvinyl alcohol PVA (average molecular weight 10 000 amu, 85% hydrolysed) solutions in de-ionised water were drop-casted on to clean glass slides to form wet PVA films. 50 μm-thick polyimide (Kapton) tapes were laid down on the glass slide first as depth gauges before the PVA solution was deposited using a second glass slide as a squeegee. A custom printing rig, consisting of a single-nozzle MicroFab printing device (80 μm nozzle diameter) was used to pattern the LC droplets on to the wet PVA film. The viscosity of the LC mixture was around 110 mPa s at 20 °C, which is significantly greater than the jetting limit of 20 mPa s suggested by the printhead manufacturer. However, extended rheological measurement of the LC mixture showed that its viscosity

[a]*Centre of Molecular Materials for Photonics and Electronics, Department of Engineering, University of Cambridge, 9 JJ Thomson Avenue, Cambridge, CB3 0FA, UK. E-mail: djg47@cam.ac.uk; hjc37@cam.ac.uk*
[b]*Inkjet Research Centre, Institute for Manufacturing, Department of Engineering, University of Cambridge, 17 Charles Babbage Road, Cambridge, CB3 0FS, UK. E-mail: imh2@cam.ac.uk; wkh26@cam.ac.uk*

decreases significantly at elevated temperature, obeying the typical Arrhenius behaviour. While commercial inkjet systems typically process inks at room or modestly elevated temperature, much higher ink temperature has been shown to be feasible for printing functional materials such as phase-change resist.[13] Therefore, the printhead was heated to 90–95 °C, close to the isotropic to nematic transition point of the LC laser mixture, to provide the optimum viscosity for printing. Individual droplet volumes were typically 200–300 pl. A custom pneumatic/vacuum controller was used to maintain the LC meniscus position at the nozzle and a bipolar waveform was applied to eject LC drops on to the wet PVA film. The experimental arrangement is depicted in Fig. 1. For comparison purposes, LC drops were jetted using similar inkjet processing conditions and depositing on to either clean, dry glass substrates or substrates coated with a planar alignment agent (Merck AM 4276) with uniaxial rubbing direction.

To measure the excitation laser threshold and the polarization of the emission from printed LC samples, coated films were photo-pumped by the second harmonic (λ = 532 nm) of a neodymium yttrium aluminium garnet (Nd:YAG) laser (Polaris II, New Wave Research), which had a 3–4 ns pulse duration and a repetition rate of 1 Hz.[9] The pump beam was focussed to a spot size of 110 μm at the sample and was left circularly polarised. The output from the LC samples was collected in the forward direction normal to the substrates (parallel to the axis of the helix) and focussed on to an HR2000 USB spectrometer (Ocean Optics, resolution 0.3 nm).

Results

Initial experiments were performed by depositing the lasing LC formulations on to cleaned, uncoated glass substrates. After printing, uniform sessile drops were obtained with a typical diameter of ≈300 μm. Photographs of the droplet profiles obtained after inkjet deposition, between crossed polarizers, are shown in Fig. 2(a). Here, it is clear that substantial non-uniformity in the LC director profile exists within the droplet. Disclination lines, representing defects in the director orientation, are also widespread across the droplet. Further non-uniformity is also visible within the droplet where there is a change in color (from red at the centre to blue at the edges) as the droplet thickness reduces toward the edge. The emission profile, after

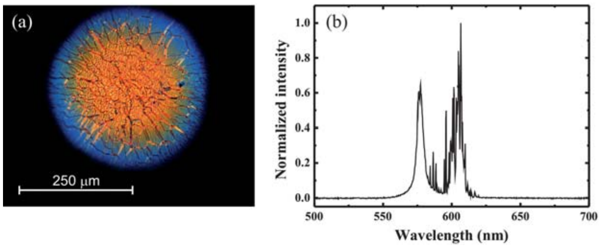

Fig. 2 Results from inkjet deposition on to a cleaned, untreated glass substrate: (a) the deposited drop profile, between crossed polarizers, showing considerable non-uniformity; (b) the multimode emission spectrum under optical excitation at a wavelength of 532 nm.

photo-pumping, is shown in Fig. 2(b). This demonstrates a strong multi-mode lasing output, characterized by a series of variable linewidth peaks between approximately 560 nm and 620 nm (corresponding to the fluorescence emission curve of PM-597). The large number of lasing modes is indicative of multiple domains within the droplet, consisting of regions with different values of the helical pitch. Previous work, in rubbed planar surface aligned LC cells, showed that multi-domain samples with slightly different pitch values, and with a typical domain size equal to or less than the pump spot size, resulted in multi-mode lasing output.[14] On the other hand, monodomain samples exhibited high quality, single mode lasing.[14] Poor emission characteristics, such as those presented in Fig. 2(b) significantly limit the scope of laser applications, which typically demand narrow linewidths centered on a well-defined emission wavelength.

To try to improve the droplet uniformity, experiments were also carried out using deposition on to surfaces treated with rubbed and baked polyimide alignment layers, which promote planar anchoring of the LC in conventional glass cells. In this case, significant wetting of the surface by the droplet was observed both immediately after deposition and as a function of time, making devices impractical.

In an attempt to combine desirable single-mode laser emission characteristics with accurate spatial positioning, we have developed an alternative deposition approach by directly printing the LC mixture on to a wet film of 10 wt% PVA polymer solution in deionized water, as illustrated in Fig. 1. Care was taken to deposit soon after film coating to ensure droplets were deposited on to wet

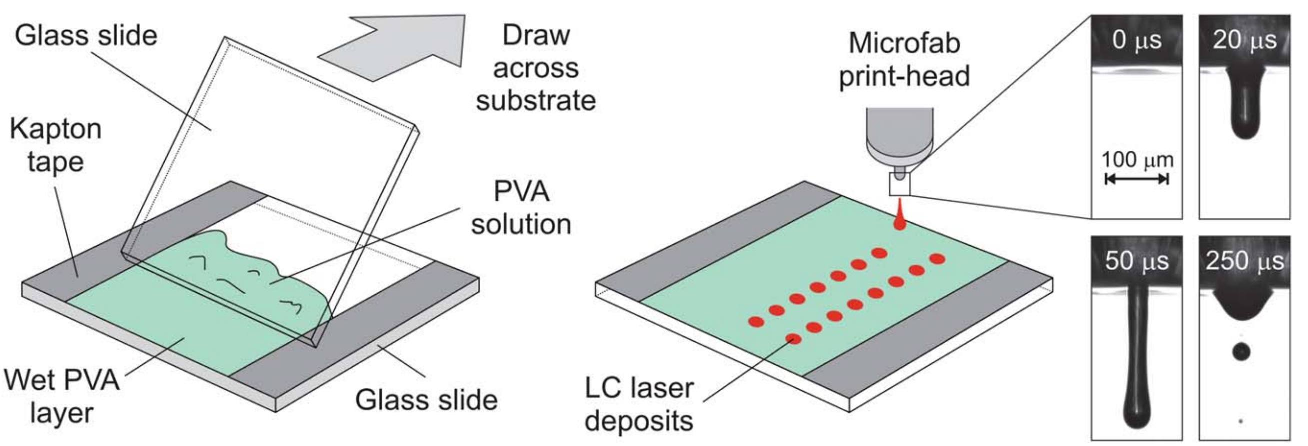

Fig. 1 Schematic of the jetting and deposition process used in the work showing (left) creation of the wet polymer (PVA) solution, deposition of lasing LC media (middle) and (right) dynamics of the inkjet droplet formation from the printhead.

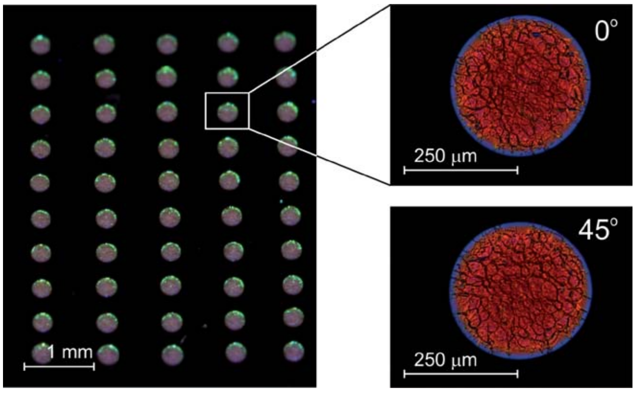

Fig. 3 Pictures of inkjet printed LC laser droplets on to a PVA film; (left) a regular array of droplets; (right) close up images (between crossed polarizers) of deposited droplets showing the rotationally invariant texture.

solution. Subsequently, films were allowed to dry completely (approximately one hour) before examining the lasing characteristics.

Fig. 3 shows an inkjet printed array of the LC droplets after printing on to the wet PVA film, and the resultant LC texture within each droplet after the film had dried. Compared to the deposition on to the untreated surface, Fig. 2, the texture in Fig. 3 possesses greater uniformity in color; this is directly attributable to a more uniform chiral nematic pitch across the droplet compared to the earlier result, Fig. 2. The texture also remains invariant under rotation by 45° (Fig. 3 (right)) between crossed polarisers, indicating that the LC profile is rotationally symmetric within the droplet itself. Furthermore, there is no optical extinction within the droplet. Combined with the fact that the material is chiral, these observations suggest that the likely LC director profile is where the helical axis is perpendicular to the substrate (Grandjean texture). Such an orientation is a prerequisite for single-mode photonic band-edge lasing in chiral LCs normal to the substrate.[2]

The key stages of a typical droplet deposition event are shown in Fig. 4 (left), which shows images captured from a high-speed camera. At 0.2 ms, the LC droplet is shown impacting the surface with subsequent deformation of both the surface and droplet. However, in the frames 0.6 ms to 500 ms, it is clear that the surface tension and immiscibility of the LC droplet to the wet PVA solution is sufficient to prevent the droplet from dispersing into the bulk polymer solution. Finally, in the 2 s frame, the droplet is shown in the equilibrium position on the surface of the film with a well-defined and symmetrical profile.

The necessary lasing alignment of the LC, in the standing helix configuration, appears to be achieved through a combination of interaction of the PVA polymer with the LC and mechanical forces occurring through deformation of the LC droplet. The interaction of PVA polymer with both nematic and chiral LCs has been examined previously in the context of polymer dispersed liquid crystal devices.[15] It was determined that PVA promotes parallel arrangement of the LC director at the interface.[16] Following the impact process depicted in Fig. 4, and the resultant lateral shear as it reaches an equilibrium state, the LC droplet adopts an oblate shape with the minor-axis perpendicular to the PVA film. It is noteworthy that the droplet does not continue to wet the surface and both the droplet shape and profile remain fixed after the film has dried. The combination of the parallel anchoring and lateral motion leads to the standing helix alignment depicted in Fig. 4 (right) and confirmed through polarizing microscopy.

Following the observation of the required chiral LC alignment, the emission characteristics of the LC lasing droplets were examined. After optical excitation at 532 nm, the resulting emission spectrum and input–output characteristics are presented in Fig. 5. From Fig. 5(a), the sample shows clear single-mode behavior with an emission peak at 580 nm, corresponding to the long-wavelength edge of the PBG and a linewidth of less than 1 nm. From the plot of the output as a function of the input energy (Fig. 5(b)), the sample exhibits a lasing threshold of $\approx$300 nJ per pulse. For conventional (non-jetted) samples, filled by capillary action into 10 μm transmissive test cells prepared with anti-parallel alignment layers, the threshold was measured to be 100 nJ per pulse. Therefore, it is expected that further reduction in the threshold, toward that measured in conventional samples, would be obtained through improved matching of the spatial pump laser profile with the LC droplet.

The polarization state of the LC laser was experimentally determined and found to be right-circularly polarized, matching the handedness of the helicoidal structure. This provides further evidence that the laser mechanism is due to the large density of states at the edge of the PBG.[17] The narrow linewidth of the lasing output would appear to be a direct consequence of the significant improvement in droplet uniformity generated by this inkjet deposition technique.

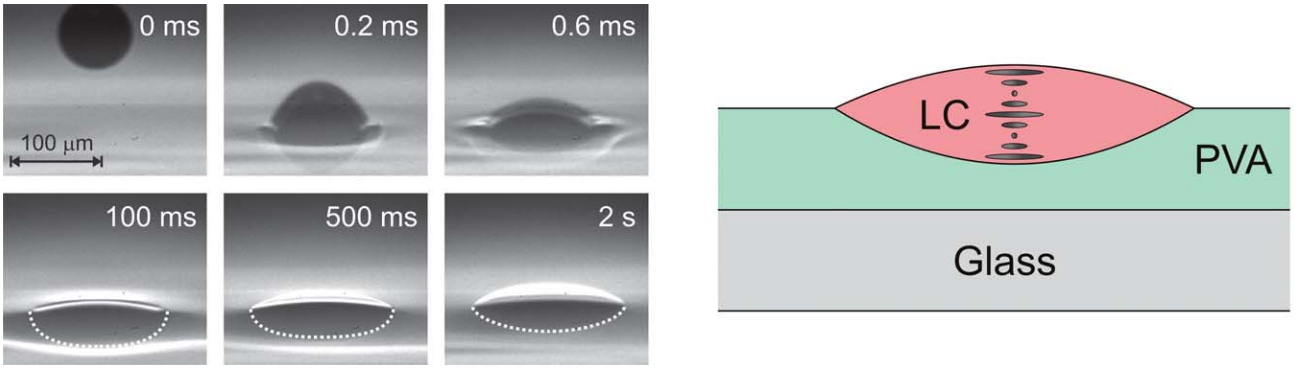

Fig. 4 High-speed camera images of the droplet impact process (left) and pictorial representation of the sample cross-section (right) with the chiral LC in the Grandjean, or standing helix, alignment.

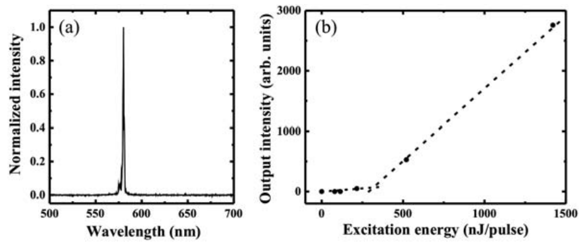

Fig. 5 (a) Laser emission following optical excitation at the absorption maximum of the laser dye and (b) output intensity as a function of excitation energy showing well-defined lasing threshold.

It is expected that complex and functional laser arrays, created by this printed LC technique, will have important potential in a variety of technological areas. The combination of the high degree of positioning and control of the lasing emission characteristics, continuously selectable in the range 450–850 nm with very narrow linewidths,[18] would permit new applications of the technology. Arrays of inkjet printed LC lasers could also be combined with array-based pumping techniques[19] for the generation of multiple simultaneous lasers, of arbitrary wavelengths, within a single substrate. Of particular interest would be lab-on-a-chip applications such as fluorescence tag-based bio-assays, for example, whereby arrays of independently configurable lasers could be printed into sample wells for simultaneous optical analysis.

Other applications could include micro-optical sources or in information display, for example; especially if the jetted droplet dimensions could be reduced to around 10 μm currently obtainable with state of the art printheads.[11] Work is also in progress to examine encapsulation and alternative polymeric solutions for increased functionality and environmental ruggedness.

Conclusion

In this communication, we have demonstrated a method to create reproducible multiple low threshold single-mode laser devices by precision inkjet deposition of the LC lasing medium on to wet, solution-processible PVA films. These printed lasers retain all the emission characteristics of laser sources but with the simplicity and advantages of inkjet printing. A combination of interfacial interaction, promoting planar alignment of the LC director, and mechanical forces originating during the deposition process promote the standing helix alignment required for photonic band-edge lasing to occur normal to the glass substrate.

Acknowledgements

We acknowledge the Engineering and Physical Sciences Research Council (UK) for financial support through the Technology Translation Grant (Coherent Optical Sources using Micromolecular Ordered Structures), EP/H046658/1 and Innovation in Industrial Inkjet Technology, EP/H018913/1. One of the authors (SMM) gratefully acknowledges financial support from The Royal Society. The authors also wish to acknowledge Dr Clare Conboy of Printed Electronics Ltd for dynamic rheology measurements.

References

1 D. K. Yang, X. Y. Huang and Y. M. Zhu, *Annu. Rev. Mater. Sci.*, 1997, **27**, 117–146.
2 H. Coles and S. Morris, *Nat. Photonics*, 2010, **4**, 676–685.
3 P. J. Collings and M. Hird, *Introduction to Liquid Crystals: Chemistry and Physics*, Taylor and Francis, London, 1997.
4 V. I. Kopp, B. Fan, H. K. M. Vithana and A. Z. Genack, *Opt. Lett.*, 1998, **23**, 1707–1709.
5 C. Mowatt, S. M. Morris, T. D. Wilkinson and H. J. Coles, *App. Phys. Lett.*, 2010, **97**, 251109.
6 A. Chanishvili, G. Chilaya, G. Petriashvili, R. Barberi, R. Bartolino, G. Cipparrone, A. Mazzulla, R. Gimenez, L. Oriol and M. Pinol, *Appl. Phys. Lett.*, 2005, **86**, 051107.
7 P. J. W. Hands, C. A. Dobson, S. M. Morris, M. M. Qasim, D. J. Gardiner, T. D. Wilkinson and H. J. Coles, *Proc. SPIE*, 2011, **8114**, 81140T.
8 K. Sonoyama, Y. Takanishi, K. Ishikawa and H. Takezoe, *Jpn. J. Appl. Phys., Part 2*, 2007, **46**, 874–876.
9 D. J. Gardiner, S. M. Morris, P. J. W. Hands, C. Mowatt, R. Rutledge, T. D. Wilkinson and H. J. Coles, *Opt. Express*, 2011, **19**, 2432–2439.
10 P. J. W. Hands, D. J. Gardiner, S. M. Morris, C. Mowatt, T. D. Wilkinson and H. J. Coles, *Appl. Phys. Lett.*, 2011, **98**, 141102.
11 K. K. B. Hon, L. Li and I. M. Hutchings, *CIRP Ann.*, 2008, **57**, 601–620.
12 G. D. Martin, S. D. Hoath and I. M. Hutchings, *J. Phys.: Conf. Ser.*, 2008, **105**, 012001.
13 W. K. Hsiao, S. D. Hoath, G. D. Martin and I. M. Hutchings, *J. Imaging Sci. Technol.*, 2009, **53**, 0503041–0503048.
14 S. M. Morris, A. D. Ford, B. J. Broughton, M. N. Pivnenko and H. J. Coles, *Proc. SPIE*, 2005, **5741**, 118–127.
15 P. S. Drzaic, *Liquid Crystal Dispersions*, World Scientific, Singapore, 1995.
16 P. S. Drzaic and A. Muller, *Liq. Cryst.*, 1989, **5**, 1467–1475.
17 J. Schmidtke and W. Stille, *Eur. Phys. J. B*, 2003, **31**, 179–194.
18 S. M. Morris, P. J. W. Hands, S. Findeisen-Tandel, R. H. Cole, T. D. Wilkinson and H. J. Coles, *Opt. Express*, 2008, **16**, 18827–18837.
19 P. J. W. Hands, S. M. Morris, T. D. Wilkinson and H. J. Coles, *Opt. Lett.*, 2008, **33**, 515–517.